EurJIC European Journal of Inorganic Chemistry

FULL PAPER

DOI: 10.1002/ejic.201200535

The Reduction of Sterically Hindered *o*-Quinone and *o*-Iminoquinone with Gallium and "GaI"

Alexandr V. Piskunov,*[a] Arina V. Maleeva,[a] Irina N. Mescheryakova,[a] and Georgii K. Fukin[a]

Dedicated to Professor Gleb A. Abakumov on the occasion of his 75th birthday

Keywords: Gallium / Quinones / Reduction / EPR spectroscopy

Metallic gallium reacts with 3,6-di-*tert*-butyl-*o*-benzoquinone (**3,6-Q**) in THF to produce a gallium tris-*o*-semiquinolate complex, whereas the same interaction with 4,6-di-*tert*-butyl-*N*-(2,6-diisopropylphenyl)-*o*-iminobenzoquinone (**imQ**) does not proceed. The reduction of **imQ** is possible with amalgamed gallium in THF and produces a gallium complex that contains two *o*-iminobenzoquinone ligands in different redox states. In the case of **3,6-Q**, the analogous reaction leads to dimeric derivative $[Cat_2Ga(Et_2O)_2]$-[CatGa] (in which Cat is the dianion of **3,6-Q**). The structure of this compound was determined by X-ray diffraction analysis. The gallium(III) amidophenolate derivative can only be obtained by exchange reaction of $APNa_2$ with GaI_3 (in which AP is the dianion of **imQ**). The reduction of **3,6-Q** and **imQ** with "GaI" results in the formation of corresponding compounds that contain redox-active ligands in the dianionic state. The structure of $[AP_2Ga][GaI_2]$ was determined by X-ray diffraction analysis.

Introduction

The utility of transition and noble metals in catalytic processes derives from their ability to be involved in the electron-transfer reactions. In principle, such reactivity can be simulated for non-transition-metal complexes with redox-active ligands (*o*-quinones, *o*-iminoquinones, *α*-diimines).[1] These derivatives are able to participate in oxidative addition[2] or reductive elimination[3] reactions in which the electron transfer is realized not on account of the metal ion but the redox-active ligand. Therefore such compounds exhibit various interesting reactivity towards different substrates. Recently the facile addition of alkynes to the gallium complex that contains the 1,2-bis[(2,6-diisopropylphenyl)imino]acenaphthene (BIAN) ligand and an unusual thermally induced elimination of this alkyne accompanied by C–C and C–Ga bond cleavage were discovered (Scheme 1).[4a] This interaction forms the basis for involving (BIAN)Ga–Ga(BIAN) in the catalytic hydroamination reaction.[4b]

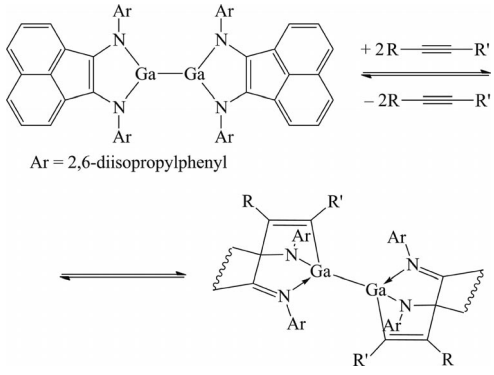

Scheme 1. The reaction of digallane with alkynes.

Group III metal complexes (including gallium derivatives) based on quinone ligands were obtained as a result of the reaction of different quinones (**Q**) with metal halides for the first time.[5] The **Q** was found to be able to oxidize the halide anion with the subsequent formation of paramagnetic metal complexes of the type $SQMHal_2$ (SQ is the radical anion of **Q**). They were characterized using EPR spectroscopy. Gallium compounds of this type can be also obtained by the direct addition of iodine to the reaction mixture of metal and quinone or by the exchange interaction of an equimolar quantity of alkali-metal quinoid salt and GaI_3.[6] Moreover, unstable paramagnetic mono-*o*-semiquinolate gallium complexes form as a result of the reaction of *o*-quinones with $GaEt_3$.[7]

[a] G.A. Razuvaev Institute of Organometallic Chemistry, Russian Academy of Sciences,
49 Tropinina Street, 603950 Nizhny Novgorod, Russian Federation
Fax: +7-831-4627497
E-mail: pial@iomc.ras.ru
Homepage: www.iomc.ras.ru

One of the most convenient methods of synthesis of metal complexes with redox-active ligands is the direct reduction of *o*-quinones and their hetero-analogues by metals or metal amalgams.[8] (BIAN)Ga–Ga(BIAN)[9a] and the tris-*o*-semiquinolate gallium(III) derivatives that contain different *o*-quinones were synthesized by this method.[6,9b–9d] In some cases, the direct interaction of quinones with gallium leads to the formation of the respective dianionic catecholate derivatives. As reported in the literature,[6] heating of the gallium metal with 1,2-naphthoquinone (**NQ**) in refluxing toluene results in a deeper reduction of **NQ** and gives the dimeric catecholate complex $[Ga^{II}(NCat)]_2$ (NCat is the dianion of **NQ**). Catecholate gallium derivatives $[(Hal_4Cat)Ga^{II}\cdot(phen)]_2$ (Hal_4Cat are dianions of tetrahalo-substituted *o*-quinones **Hal_4Q**; phen = 1,10-phenanthroline) form as the result of the reaction of metal with quinones in the presence of phen.[10a] Unfortunately, the authors[6,10a] did not produce sufficient evidence of such structures, and the last ones are questionable. Moreover, the minor product obtained in the reaction of **Cl_4Q** with Ga in the presence of phen is the structurally characterized monomeric complex $(Cl_4Cat)GaCl\cdot py\cdot phen$ (py = pyridine).[10b] It indicates the more complicated nature of the interaction of metallic gallium with **Hal_4Q**, which includes elimination of halides from the initial *o*-quinone.

Low-oxidation-state metal derivatives are widely known to reduce 1,2-diketones and related ligands to give chelated compounds with reduced forms of the redox-active ligands. Thus the interaction of benzil with "GaI" results in the formation of a novel trimetallic bis(enediolato) complex.[11a] "GaI" was shown to be a convenient initial reagent for the synthesis of α-diimine gallium derivatives.[11b–11e] The reduction of *N*-substituted diazabutadienes (DAD) or the BIAN ligand by "GaI" leads to compounds that contain the redox-active ligand in radical-anion form. They are of the type $I_2Ga(DAD)^{-\cdot}$ or $[IGa(DAD)^{-\cdot}]_2$ depending on the nature of the N-substituents.[11b–11e] The similar reaction of "GaI" with iminopyridine results in the C–C coupling of the mono-reduced organic ligand and leads to the diamagnetic dinuclear gallium compound.[11d] A recent investigation shows that the "GaI" is able to reduce aryl-substituted bis(imino)pyridine to produce paramagnetic $[2,6\text{-}(DippN{=}CPh)_2(NC_5H_3)]GaI_2$ derivative.[11f]

The reactivity of gallium or "GaI" towards *o*-iminoquinones currently has not been investigated. All known *o*-iminoquinonato gallium complexes are tris-*o*-iminobenzosemiquinolates, which were obtained in the reaction of 2-(3,5-di-R-anilino)-4,6-di-*tert*-butylphenol (R = *t*Bu, CF_3, Cl; 3 equiv.) with $GaCl_3$ (1 equiv.) in the presence of Et_3N and air oxygen.[12a] The similar gallium complex with R = OCH_3 undergoes intramolecular coupling of *o*-iminosemiquinones with the formation of the new paramagnetic hexadentate ligand.[12b]

Despite the variety of knowledge about gallium complexes that contain different redox-active ligands that is available to date, the information presented above seems slightly discrepant and incomplete. A number of *o*-quinolate compounds were not isolated in the individual state, or their structure was not proven unambiguously. The present work is devoted to the deeper investigation of gallium complexes based on *o*-benzoquinone and *o*-iminobenzoquinone ligands.

Results and Discussion

The direct interaction of *o*-quinones and *o*-iminoquinones with metals or amalgamated metals was shown to be a convenient method for the synthesis of their corresponding derivatives.[8] Tris(3,6-di-*tert*-butyl-*o*-benzosemiquinolato)gallium(III) (**1**) was generated in solution over the course of the reaction between gallium and **3,6-Q** for the first time.[9b] Later this compound was obtained by a more time-consuming exchange interaction.[13] We have found that the reaction of **3,6-Q** with an excess amount of gallium in THF results in the formation of **1** with a quantitative yield (Scheme 2, path a).

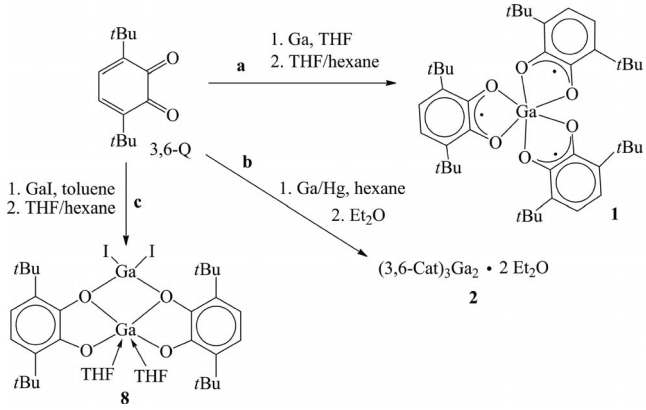

Scheme 2. The synthesis of gallium(III) derivatives based on the **3,6-Q** ligand.

The use of amalgamated gallium in the reaction with **3,6-Q** allows one to carry out the process in a hydrocarbon medium and perform the deeper reduction of the initial *o*-quinone. The gallium(III) catecholate complex was obtained in hexane as a result (Scheme 2, path b). Removal of hexane and treatment of the solid residue with diethyl ether results in the formation of crystalline product **2**. The last was characterized by elemental analysis, IR and ^1H NMR spectroscopy, and X-ray diffraction analysis.

According to ^1H NMR spectroscopy data (Figure 1, A), the ratio between catecholate ligands and diethyl ether molecules coordinated to the metal center in **2** is 3:2. Moreover, a considerable asymmetrical assignment of electron density in catecholate ligands was observed. The signals at δ = 1.31 and 1.47 ppm correspond to the protons of inequivalent *tert*-butyl groups. The doublets at δ = 6.86 and 6.79 ppm are attributed to the inequivalent protons of the aromatic ring. The value of the spin–spin interaction constant ($J_{H,H}$ = 8.5 Hz) is typical for derivatives of benzenes that contain *ortho*-protons. The analysis of the integral intensity of signals in the ^1H NMR spectrum indicates that complex **2** has the following composition: $(3,6\text{-Cat})_3Ga_2\cdot 2Et_2O$. It is in good agreement with cryoscopic (C_6H_6) mo-

lecular-weight measurements (956 g mol^{-1} versus calcd. 948.6 g mol^{-1}) for complex **2**. Given the above, it is possible to suppose the structure of complex **2** in which the environment of the first gallium atom is formed by three catecholate ligands, whereas the second metal atom is coordinated to the three oxygen atoms of diolate ligands and to two diethyl ether molecules (Scheme 3).

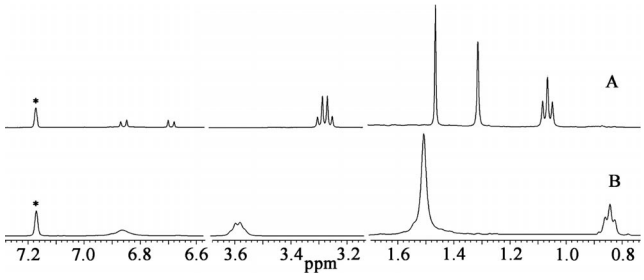

Figure 1. The ^{1}H NMR spectra of gallium(III) catecholate complexes (A) **2** and (B) **3** in C_6D_6. The asterisk (*) indicates the residual solvent peak.

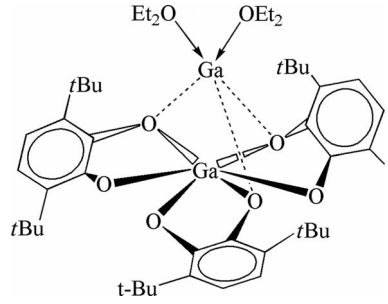

Scheme 3. The expected structure of complex **2**.

The ^{1}H NMR spectrum of gallium catecholate derivative **2** changes over time. The gradual disappearance of spectrum A and the appearance of spectrum B is observed in C_6D_6 solution (Figure 1). This fact indicates the transformation of complex **2** in solution. Actually, the long-continued recrystallization of **2** from a mixture of Et_2O and hexane results in the formation of crystalline product **3**. The ^{1}H NMR spectrum of **3** coincides completely with the spectrum of compound **2** after its long-term storage in C_6D_6 solution (Figure 1, B).

The elemental analysis and cryoscopic (C_6H_6) molecular-weight determination data for complexes **2** and **3** indicates that these compounds have the same composition. The ^{1}H NMR spectrum of **3** (Figure 1, B) contains a singlet signal of *tert*-butyl group protons and a singlet signal of aromatic ring protons. All signals are considerably broadened. This fact indicates that there is a dynamics of coordination sphere in solution of complex **3**, and protons of catecholate ligands become practically equivalent as the result. It is necessary to note that the transformation of **2** into **3** is irreversible. The repeated recrystallization of **3** from diethyl ether does not change the spectroscopic data of the resulting compound.

The structure of complex **3** was determined by X-ray diffraction analysis (Figure 2). The molecule of **3** consists of two gallium atoms with different coordination geometry. Ga(1) has a distorted tetrahedral environment formed by oxygen atoms O(1) and O(2) of one catecholate ligand and O(3) and O(6) of another two diolate ligands. The distorted octahedral coordination sphere of the Ga(2) atom includes the O(3), O(4), O(5), O(6), O(7), and O(8) atoms of two catecholate ligands and two diethyl ether molecules. The O(3), O(6), O(7), and O(8) atoms form the equatorial plane, whereas O(4) and O(5) atoms occupy apical positions. The values of the C–O and C–C bond lengths of *o*-quinonate fragments indicate the catecholate nature of the redox-active ligands. It is necessary to note that the O(3)–C(15) and O(6)–C(34) bonds [1.414(2) and 1.406(2) Å, respectively] are longer than the O(1)–C(1), O(2)–C(2), O(4)–C(16), and O(5)–C(29) (1.36–1.38 Å) bonds. The values of the Ga(1)–O(3,6) and Ga(2)–O(3,6) distances [1.877(11)–1.9067(9) and 2.0655(11) Å, respectively] are appreciably more than the values of Ga(1)–O(1,2) [1.8105(11)–1.8146(11) Å] and Ga(2)–O(4,5) [1.8667(11)–1.8771(11) Å] bond lengths. These facts are a result of bridge-type Ga(1,2)–O(3,6) bonds. The interatomic Ga(1)···Ga(2) distance is 2.8813(2) Å and exceeds the sum of covalent radii for these atoms (2.59 Å).[14] The dihedral angles between the central Ga(1)O(3)Ga(2)O(6) metallocycle and catecholate ligands are 77.6–89.4°. It minimizes the nonbonding interactions in **3**. Selected bond lengths and angles in complex **3** are given in Table 1. The crystal data collection and structure refinement data are listed in Table 3.

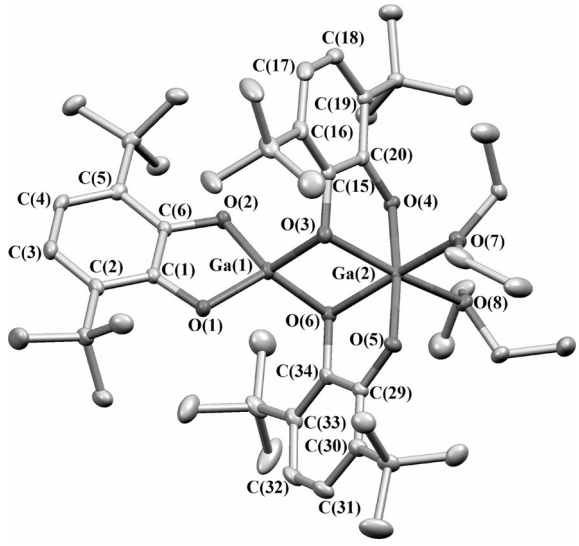

Figure 2. The molecular structure of complex **3** with 30% thermal probability ellipsoids. Hydrogen atoms are omitted for clarity.

In contrast to **3,6-Q**, the interaction of metallic gallium with 4,6-di-*tert*-butyl-*N*-(2,6-diisopropylphenyl)-*o*-iminobenzoquinone (**imQ**) does not proceed. The use of amalgamated gallium in the reaction with **imQ** in THF allows one to obtain only the mixed-ligand derivative of Ga^{III} (**4**) in which the first **imQ** ligand has a radical-anionic and the second one a dianionic nature (Scheme 4, path a). The pres-

Table 1. Selected bond lengths [Å] and angles [°] of complex **3**.

Bond	[Å]	Angle	[°]
C(1)–O(1)	1.3748(19)	O(1)–Ga(1)–O(2)	94.21(5)
C(6)–O(2)	1.3850(18)	O(1)–Ga(1)–O(3)	118.42(5)
C(1)–C(2)	1.402(2)	O(2)–Ga(1)–O(3)	120.97(5)
C(2)–C(3)	1.389(3)	O(1)–Ga(1)–O(6)	115.89(5)
C(3)–C(4)	1.397(3)	O(2)–Ga(1)–O(6)	118.39(5)
C(4)–C(5)	1.395(2)	O(3)–Ga(1)–O(6)	91.16(4)
C(5)–C(6)	1.391(2)	O(4)–Ga(2)–O(5)	173.78(4)
C(6)–C(1)	1.412(2)	O(4)–Ga(2)–O(7)	94.80(5)
Ga(1)–O(1)	1.8105(11)	O(5)–Ga(2)–O(7)	88.75(5)
Ga(1)–O(2)	1.8146(11)	O(4)–Ga(2)–O(8)	89.95(4)
Ga(1)–O(3)	1.8747(11)	O(5)–Ga(2)–O(8)	95.09(4)
Ga(1)–O(6)	1.9067(9)	O(7)–Ga(2)–O(8)	91.07(4)
Ga(2)–O(3)	2.0655(9)	O(3)–Ga(2)–O(4)	82.33(4)
Ga(2)–O(4)	1.8667(11)	O(3)–Ga(2)–O(5)	92.28(4)
Ga(2)–O(5)	1.8771(11)	O(3)–Ga(2)–O(7)	95.25(4)
Ga(2)–O(6)	2.0655(11)	O(3)–Ga(2)–O(8)	170.39(5)
Ga(2)–O(7)	2.0391(11)	O(4)–Ga(2)–O(6)	94.41(5)
Ga(2)–O(8)	2.0448(9)	O(5)–Ga(2)–O(6)	81.69(5)
O(3)–C(15)	1.414(2)	O(6)–Ga(2)–O(7)	169.80(5)
O(4)–C(20)	1.3625(16)	O(6)–Ga(2)–O(8)	93.30(4)
O(5)–C(29)	1.3610(17)	O(3)–Ga(2)–O(6)	81.66(4)
O(6)–C(34)	1.406(2)	Ga(1)–O(3)–Ga(2)	93.86(4)
Ga(1)···Ga(2)	2.8813(2)	Ga(1)–O(6)–Ga(2)	92.91(4)

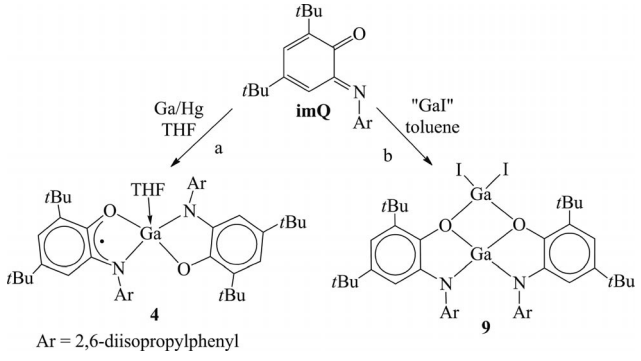

Scheme 4. The synthesis of gallium(III) derivatives based on the **imQ** ligand.

ence of two differently charged *o*-iminoquinonate ligands in complex **4** is clear from analysis of its EPR spectrum. The hyperfine structure of the EPR spectrum of **4** in THF arises from hyperfine coupling (HFC) of unpaired electron with magnetic nuclei ^{69}Ga (60.1%, I = 3/2, μ_N = 2.01659),[15] ^{71}Ga (30.9%, I = 3/2, μ_N = 2.56227),[15] two equivalent protons ^{1}H (99.98%, I = 1/2, μ_N = 2.7928),[15] and two equivalent nitrogen atoms ^{14}N (99.63%, I = 1, μ_N = 0.4037)[15] of both *o*-iminoquinonate ligands. The splitting parameters are $a_i(^2H)$ = 2.37 G, $a_i(^{14}N)$ = 3.40 G, $a_i(^{69}Ga)$ = 13.28 G, $a_i(^{71}Ga)$ = 16.88 G, and g_i = 2.0033 (Figure 3, A). The equivalence of two protons and two nitrogen atoms and the values of HFC constants that are two times less than the corresponding HFC constants in mono-*o*-iminosemiquinonato complexes[16] indicate the fast migration (on the EPR timescale) of unpaired electron between *o*-iminoquinonato ligands.

The similar delocalization of unpaired electron was reported for related five-coordinate tin[2f] and germanium[17] complexes that contain two differently charged *o*-iminoquinonate ligands. The mixed-ligand gallium(III) derivatives that contain radical-anion and dianion forms of *o*-quinone simultaneously were also described.[9,13] They form as the result of a displacement of one SQ ligand from the initial tris-*o*-semiquinolate complex by two 3-butylpyridine molecules[9] or as the result of an exchange reaction between an equimolar quantity of GaI_3 and mono- and dithallium *o*-quinonate salts in the presence of tetramethylethylenediamine.[13]

The removal of THF from the solution of **4** and redissolution of the residue in hexane leads to changes in the EPR spectrum (Figure 3). The hyperfine structure of the EPR signal registered in hexane shows the interaction of unpaired electrons with magnetic nuclei of one *o*-iminoquinonate ligand only [$a_i(^1H)$ = 4.37 G, $a_i(^{14}N)$ = 6.04 G, $a_i(^{69}Ga)$ = 11.95 G, $a_i(^{71}Ga)$ = 15.19 G, g_i = 2.0028] (Figure 3). In addition, the values of hyperfine coupling con-

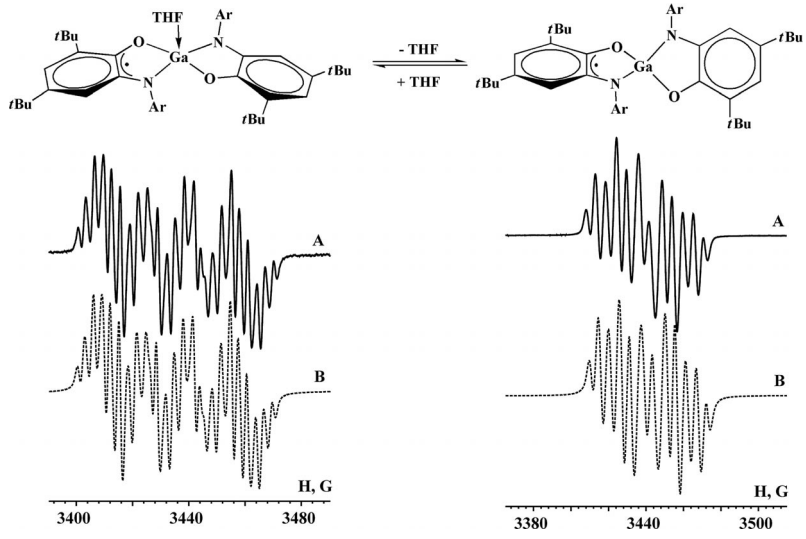

Figure 3. The EPR spectra of complexes [APGa(imSQ)(THF)] (**4**) in THF (on the left) and [APGa(imSQ)] (**5**) in hexane (on the right) (A: experimental, B: simulated).

stants $a_i(^1H)$ and $a_i(^{14}N)$ in hexane are nearly twice as large as the respective spectrum parameters in THF solution. Changes described above can be explained by the following. The reaction of amalgamated gallium with **imQ** results in the formation of the five-coordinated derivative **4** that contains weakly coordinated THF molecules. The decoordination of THF from the gallium atom in hexane solution of **4** takes place. It leads to the generation of four-coordinate Ga^{III} derivative [APGa(imSQ)] (**5**) (Figure 3). It is accompanied by the organization of the distorted tetrahedral coordination geometry around the Ga^{III} center. Such geometry prevents the delocalization of unpaired electron between two *o*-iminoquinonate ligands. A similar situation takes place in tetrahedral gallium(III) derivatives that contain two differently charged diazabutadiene ligands.[18] Therefore there is a radical center delocalization over two **imQ** ligands in complex **4**, whereas in **5** the unpaired electron localizes over one ligand only. Unfortunately, we could not isolate complexes **4** and **5** in their individual states. But treatment of **5** with pyridine (py) allows one to obtain the crystalline product **6** (Scheme 5).

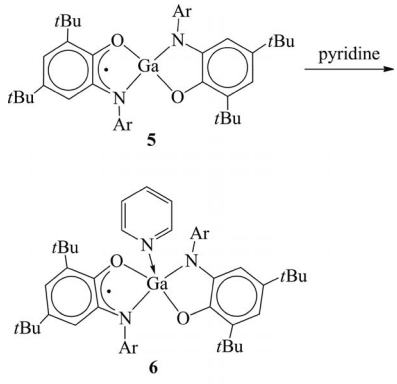

Scheme 5. The synthesis of [APGa(imSQ)(py)] (**6**).

In compliance with EPR spectroscopy data, the structure of compound **6** is similar to the structure of **4**. The EPR signal of a solution of [APGa(imSQ)(py)] (**6**) in toluene arises from the HFC of unpaired electron with magnetic nuclei of the metal atom and both **imQ** ligands. However, the EPR spectrum of **6** is characterized by broader lines than the spectrum of complex **4**. It is explained by the presence of interaction of unpaired electron with the magnetic nucleus ^{14}N of the pyridine molecule. This weak HFC makes a contribution to the value of the line width. The splitting parameters of the EPR spectrum of complex **6** are $a_i(2^1H)$ = 2.40 G, $a_i(2^{14}N)$ = 3.40 G, $a_i(^{14}N)$ = 0.60 G, $a_i(^{69}Ga)$ = 13.10 G, $a_i(^{71}Ga)$ = 16.65 G, g_i = 2.0041 (Figure 4).

In contrast to compound **4**, the dissociation of the solvent molecule from the metal center in **6** does not occur in toluene or hexane solution, and the transformation represented in Scheme 5 is irreversible. Complex **6** is characterized by a low-energy band (ca. 2010 nm) in the NIR spectrum that indicates the electron-charge transfer (ligand-to-ligand charge transfer, LLCT) between ligands in different oxidation states.

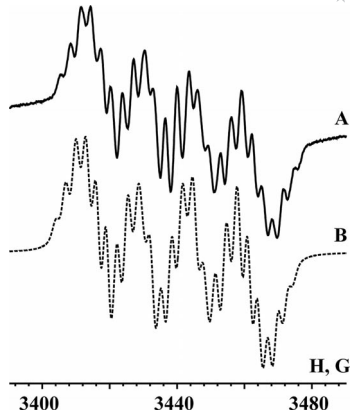

Figure 4. The EPR spectra of complex [APGa(imSQ)(py)] (**6**) in toluene (A: experimental, B: simulated).

As mentioned above, the direct interaction of **imQ** with amalgamated gallium does not result in full reduction of the redox-active ligand. Therefore the exchange reaction of disodium *o*-iminobenzoquinone salt $APNa_2$ with GaI_3 was used to obtain diamagnetic gallium(III) *o*-amidophenolate derivative **7** (Scheme 6).

$$3APNa_2 + 2GaI_3 \xrightarrow[-6NaI]{THF} \underset{\mathbf{7}}{AP_3Ga_2(THF)_2}$$

Scheme 6. The synthesis of $[AP_3Ga_2(THF)_2]$ (**7**).

In accordance with the ^1H NMR spectroscopy data of **7**, all of the *o*-amidophenolate ligands are equivalent to each other in the coordination sphere of gallium (Figure 5).

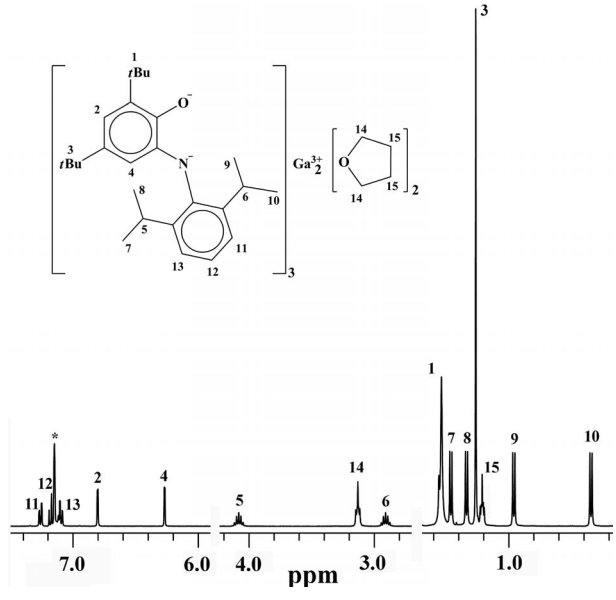

Figure 5. The ^1H NMR spectrum of **7** in C_6D_6. The asterisk (*) indicates the residual peak of the solvent.

The isopropyl groups and the protons of *N*-aryl rings are inequivalent. It results in four doublets of methyl (*i*Pr) protons (7–10), two pseudoseptets of methine protons (5

and 6), and three multiplets attributed to *N*-aryl ring protons (11–13). In addition, there are the signals of the protons of THF molecules (14 and 15) in the ^{1}H NMR spectrum. The analysis of signal intensities shows that the ratio between *o*-amidophenolate ligands and solvent molecules is 3:2. The value of chemical shifts indicates that THF molecules are coordinated to the metal atom.

On the basis of the ^{1}H NMR spectroscopy data, we can suggest a possible structure for complex **7** (Scheme 7). The first gallium atom is hexacoordinate. Three *o*-amidophenolate ligands provide a distorted trigonal prismatic environment of this metal atom. The second metal atom is coordinated by three *o*-amidophenolate oxygen atoms and two THF molecules.

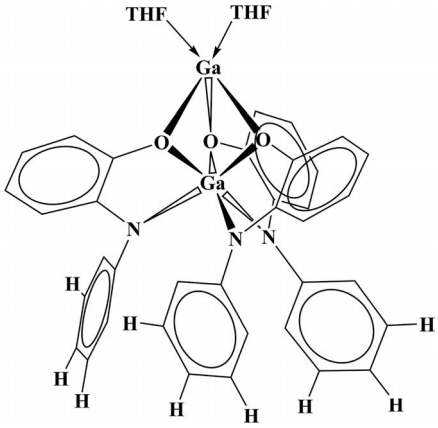

Scheme 7. The expected structure of **7**. Hydrogen atoms, isopropyl, and *tert*-butyl groups are omitted for clarity.

It is necessary to note that the structure of complex **7** is similar to the structure suggested for catecholate derivative **2**. However, the ^{1}H NMR spectrum of **7** does not change over time. This fact indicates that the structure of Ga^{III} *o*-amidophenolate compound **7** is invariable, whereas its *o*-quinone analogue **2** transforms into complex **3** in solution.

A convenient method of synthesis of metal complexes that contain a redox-active ligand in the dianionic state is the reduction of *o*-quinone (*o*-iminoquinone) by low-oxidation-state metal halides as well. Thus the interaction of **3,6-Q** and **imQ** with "GaI" results in the formation of gallium(III) catecholate and *o*-amidophenolate complexes **8** and **9**, respectively (Scheme 2, path c; Scheme 4, path b).

The ^{1}H NMR spectrum of compound **8** is characterized by broadened signals of catecholate ligand protons and is similar to the spectra of known related aluminum[19a] and indium[19b] complexes. The last ones were found to have a dimeric structure in accordance with X-ray diffraction analysis data. Hence it was supposed that **8** has a similar dimeric structure.

The structure of complex **9** was determined by X-ray diffraction (Figure 6). Selected bond lengths and angles for complex **9** are given in Table 2. The compound is binuclear and contains two gallium atoms, two *o*-amidophenolate ligands, and two iodine atoms. Each metal atom has a distorted tetrahedral environment. The apexes of tetrahedrons are formed by O(1), O(2), I(1), and I(2) atoms for Ga(1), and O(1), N(1), O(2), and N(2) atoms for Ga(2). The Ga(1), O(1), Ga(2), and O(2) atoms form the distorted rhomb. The dihedral angles between the planes of two *o*-amidophenolate ligands and the Ga(1)O(1)Ga(2)O(2) plane are 52.45 and 56.51°, respectively. The dihedral angle between C_6H_2NO fragments of two **imQ** ligands is 75.64°. The distance between Ga(1) and Ga(2) atoms is 2.8743(5) Å, and this value considerably exceeds the sum of gallium covalent radii (2.5 Å).[14] The nonbonding repulsion between metal atoms causes the deviation of the Ga(2) atom from chelate cycles. The deviations of Ga(2) from the $C_6H_2N(1)O(1)$ and $C_6H_2N(2)O(2)$ planes are 0.091 and 0.156 Å, respectively. The C–O [1.412(3)–1.413(3) Å] and C–N [1.403(3)–1.408(3) Å] bond lengths are typical for dianionic types of **imQ** ligand.[20] The C–C distances in six-membered carbon cycles of both *o*-amidophenolate ligands were averaged [1.394(4)–1.410(4) Å]. The values of Ga–O [1.9622(19)–1.9668(19) Å] and Ga–N [1.823(2)–1.826(2) Å] bond

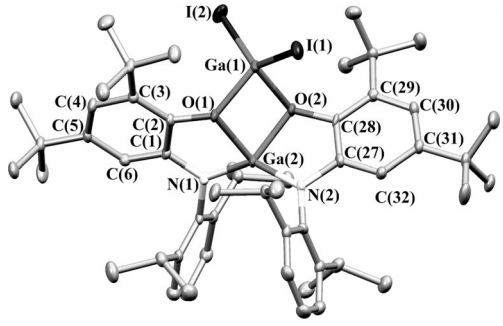

Figure 6. The molecular structure of complex **9** with 50% thermal probability ellipsoids. Hydrogen atoms are omitted for clarity.

Table 2. Selected bond lengths [Å] and angles [°] of complex **9**.

Bond	[Å]	Angle	[°]
Ga(1)–O(1)	1.9309(19)	O(1)–Ga(1)–I(2)	109.59(6)
Ga(1)–O(2)	1.955(2)	I(2)–Ga(1)–I(1)	129.035(16)
Ga(1)–I(1)	2.4660(4)	I(1)–Ga(1)–O(2)	110.08(6)
Ga(1)–I(2)	2.4809(4)	O(1)–Ga(1)–O(2)	85.68(8)
Ga(2)–O(1)	1.9622(19)	O(1)–Ga(1)–I(1)	108.40(6)
Ga(2)–O(2)	1.9668(19)	O(2)–Ga(1)–I(2)	105.46(6)
Ga(2)–N(1)	1.826(2)	O(1)–Ga(2)–O(2)	84.53(8)
Ga(2)–N(2)	1.823(2)	O(1)–Ga(2)–N(1)	87.69(9)
Ga(1)···Ga(2)	2.8743(5)	N(1)–Ga(2)–N(2)	139.25(11)
O(1)–C(2)	1.413(3)	O(2)–Ga(2)–N(2)	87.45(9)
N(1)–C(1)	1.403(3)	O(1)–Ga(2)–N(2)	123.38(10)
C(1)–C(2)	1.410(4)	N(1)–Ga(2)–O(2)	124.40(10)
C(2)–C(3)	1.399(4)	Ga(1)–O(1)–Ga(2)	95.17(8)
C(3)–C(4)	1.408(4)	Ga(1)–O(2)–Ga(2)	94.26(8)
C(4)–C(5)	1.384(4)		
C(5)–C(6)	1.392(4)		
C(1)–C(6)	1.392(4)		
O(2)–C(28)	1.412(3)		
N(2)–C(27)	1.408(3)		
C(27)–C(28)	1.408(4)		
C(28)–C(29)	1.394(4)		
C(29)–C(30)	1.401(4)		
C(30)–C(31)	1.391(4)		
C(31)–C(32)	1.395(4)		
C(27)–C(32)	1.395(4)		

lengths are less than the sum of the covalent radii of the corresponding elements (Ga–O 1.98 Å, Ga–N 1.99 Å[14]), which indicates the covalent nature of these bonds.

Another route to the synthesis of complexes **8** and **9** is the reaction of **3,6-Q** or **imQ** with gallium metal in the presence of a stoichiometric quantity of iodine (Scheme 8).

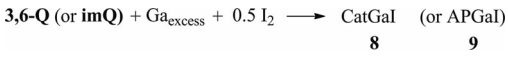

Scheme 8. An alternative synthetic method for compounds **8** and **9**.

Conclusion

The reduction of sterically hindered *o*-benzoquinone and *o*-iminobenzoquinone with metallic or amalgamated gallium as well as with "GaI" was found to be a versatile method for the synthesis of gallium complexes based on these redox-active ligands. The described reactions allow one to obtain metal derivatives that contain differently charged organic ligands depending on the reaction conditions. The structures of complexes obtained were investigated by using EPR and NMR spectroscopy, and X-ray diffraction analysis.

Table 3. Summary of crystal and refinement data for complexes **3** and **9**.

	3	**9**
Empirical formula	$C_{50}H_{80}Ga_2O_8$	$C_{52}H_{74}Ga_2I_2N_2O_2$
M_r	948.58	1152.37
Crystal system	monoclinic	monoclinic
Space group	*Cc*	$P2_1/c$
a [Å]	25.5689(14)	18.8650(10)
b [Å]	12.1796(7)	12.0855(7)
c [Å]	19.3241(11)	22.4849(12)
β [°]	121.9630(10)	92.3010(10)
V [Å^3]	5105.5(5)	5122.3(5)
Z	4	4
$D_{calcd.}$ [g cm^3]	1.234	1.494
μ [mm^{-1}]	1.104	2.297
Crystal size [mm^3]	0.69 × 0.50 × 0.11	0.37 × 0.19 × 0.10
θ Range for data collection [°]	2.54–27.00	2.00–27.00
Reflections collected	22829	45990
Independent reflections	10938	11158
Completeness to $\theta_{max.}$	99.5	99.8
Max./min. transmission	0.8882/0.5164	0.8029/0.4837
Data/restraints/parameters	10938/2/557	11158/0/562
Final *R* indices [$I > 2\sigma(I)$]	R_1 = 0.0299, wR_2 = 0.0721	R_1 = 0.0376, wR_2 = 0.0899
R indices (all data)	R_1 = 0.0338, wR_2 = 0.0736	R_1 = 0.0517, wR_2 = 0.0956
Goodness-of-fit on F^2	1.011	1.051
Largest diff. peak and hole [e Å^{-3}]	0.839 and –0.678	3.548 and –0.988

Experimental Section

General: All reactants were reagent grade. Solvents were purified by the following standard methods.[21] 3,6-Di-*tert*-butyl-*o*-benzoquinone (**3,6-Q**),[22] 4,6-di-*tert*-butyl-*N*-(2,6-diisopropylphenyl)-*o*-iminobenzoquinone (**imQ**),[23] gallium(III) iodide GaI_3,[24] and "GaI"[25] were prepared according to known procedures. All manipulations on complexes were performed under conditions in which oxygen and moisture were excluded.

The infrared spectra of complexes in the 4000–400 cm^{-1} range were recorded with an FSM 1201 Fourier-IR spectrometer in nujol. NMR spectra were recorded in C_6D_6 (for **2**, **3**, and **7**), $(CD_3)_2O$ (for **8**), or $CDCl_3$ (for **9**) with Bruker DPX-200 and Bruker Avance III 400 MHz instruments with TMS as internal standard. EPR spectra were recorded with a Bruker EMX spectrometer (working frequency ca. 9.75 GHz). The g_i values were determined by using 2,2-diphenyl-1-picrylhydrazyl (DPPH) as the reference (g_i = 2.0037). EPR spectra of **4**–**6** were simulated with WinEPR SimFonia Software (Bruker). Elemental analysis was performed with an Elemental Analyzer Euro EA 3000 instrument.

X-ray Crystallographic Study of 3 and 9: Intensity data for **3** and **9** were collected at 100(2) K with a Smart Apex diffractometer with graphite-monochromated Mo-K_α radiation (λ = 0.71073 Å) in the ϕ–ω scan mode (ω = 0.3°, 10 s on each frame). The intensity data were integrated by the SAINT program.[26] SADABS[27] was used to perform area-detector scaling and absorption corrections (semi-empirical from equivalents). The structures **3** and **9** were solved by direct methods and were refined with full-matrix least-squares on F^2 using all reflections with the SHELXTL package.[28] All non-hydrogen atoms were refined anisotropically. The hydrogen atoms were placed in calculated positions and refined in the riding model. Table 3 summarizes the crystal data and some details of the data collection and refinement for these complexes.

[(SQ)$_3$Ga] (1): A solution of **3,6-Q** (2.3 mmol, 0.5 g) in THF (30 mL) was added to the excess amount of gallium metal (12 mmol, 0.84 g). The reaction mixture was stirred and heated over 3 h, and a color change from green-red of the initial **3,6-Q** to deep green was observed. The solution was separated from the excess amount of metal and diluted with hexane. The known[13] complex **1** was obtained as a fine-crystalline deep green product after cooling; yield 0.44 g (78.0%); m.p. (dec.) > 150 °C. $C_{42}H_{60}GaO_6$ (730.65): calcd. C 69.04, H 8.28, Ga 9.54; found C 69.10, H 8.30, Ga 9.50.

[Cat$_3$Ga$_2$(Et$_2$O)$_2$] (2): A solution of **3,6-Q** (2.3 mmol, 0.5 g) in hexane (30 mL) was added to the amalgamated gallium (12 mmol, 0.84 g). The reaction mixture became bright yellow after stirring and heating over 1 h. The hexane was evaporated and the residue was recrystallized from diethyl ether. Compound **2** was obtained as colorless crystals; yield 0.47 g (65.1%); m.p. (dec.) > 120 °C. $C_{50}H_{80}Ga_2O_8$ (948.62): calcd. C 63.31, H 8.50, Ga 14.70; found C 63.45, H 8.57, Ga 14.61. ^{1}H NMR (C_6D_6, 20 °C): δ = 6.85 (d, $J_{H,H}$ = 8.5 Hz, 3 H, H_{arom}), 6.68 (d, $J_{H,H}$ = 8.5 Hz, 3 H, H_{arom}), 3.34 [q, 8 H, $CH_2(Et_2O)$], 1.46 (s, 27 H, *t*Bu), 1.31 (s, 27 H, *t*Bu), 0.97 [t, 12 H, $CH_3(Et_2O)$] ppm. IR (Nujol): $\tilde{\nu}$ = 1485 (s), 1395 (s), 1359 (s), 1306 (s), 1283 (s), 1258 (s), 1236 (s), 1219 (s), 1202 (m), 1192 (m), 1145 (s), 1091 (w), 1025 (s), 975 (s), 965 (s), 936 (m), 919 (m), 912 (m), 928 (w), 807 (s), 796 (m), 770 (m), 779 (s), 651 (s), 624 (w), 606 (w), 586 (w), 586 (w), 549 (w), 504 (w), 484 (m) cm^{-1}.

[Cat$_2$Ga(Et$_2$O)$_2$][CatGa] (3): Prolonged recrystallization of complex **2** (0.42 mmol, 0.4 g) from a mixture of Et_2O/hexane led to the formation of compound **3**; yield 0.33 g (82.4%); m.p. (dec.) > 130 °C. $C_{50}H_{80}Ga_2O_8$ (948.62): calcd. C 63.31, H 8.50, Ga 14.70; found C 63.35, H 8.52, Ga 14.67. ^{1}H NMR (C_6D_6, 20 °C): δ = 6.86 (s, 6 H, H_{arom}), 3.44 [q, 8 H, $CH_2(Et_2O)$], 1.50 (s, 54 H, *t*Bu), 0.94 [t, 12 H, $CH_3(Et_2O)$] ppm. IR (Nujol): $\tilde{\nu}$ = 1489 (s), 1399 (s), 1354 (s), 1293 (s), 1282 (s), 1262 (s), 1249 (s), 1237 (s), 1231 (s), 1219 (s),

1204 (s), 1195 (s), 1173 (m), 1159 (s), 1146 (s), 1034 (m), 1020 (s), 968 (s), 936 (s), 919 (s), 871 (s), 860 (s), 843 (m), 830 (m), 808 (s), 805 (s), 794 (s), 785 (w), 752 (s), 739 (s), 724 (s), 678 (s), 655 (s), 628 (w), 621 (w), 612 (w), 578 (m), 560 (w), 552 (m), 514 (m), 489 (s), 464 (w) cm^{-1}.

[APGa(imSQ)(py)] (6): A solution of **imQ** (1.3 mmol, 0.5 g) in THF (30 mL) was added to an excess amount of amalgamated gallium (12 mmol, 0.84 g). The reaction mixture was stirred for 2 h, and a color change from wine-red to deep green was observed. The solution was separated from metal by filtration. Pyridine (2 mL) was added to the resulted solution. Complex **6** was isolated from hexane as green-brown crystals; yield 0.4 g (68.0%); m.p. (dec.) > 170 °C. $C_{57}H_{79}GaN_3O_2$ (907.99): calcd. C 75.40, H 8.77, Ga 7.68; found C 75.45, H 8.82, Ga 7.64. IR (Nujol): $\tilde{\nu}$ = 1611 (s), 1583 (s), 1559 (m), 1533 (w), 1514 (w), 1477 (s), 1448 (s), 1435 (s), 1415 (s), 1358 (s), 1333 (s), 1321 (s), 1290 (s), 1247 (s), 1220 (w), 1211 (s), 1201 (m), 1170 (m), 1162 (w), 1105 (m), 1055 (w), 1046 (m), 1026 (w), 993 (s), 935 (w), 914 (w), 888 (w), 879 (w), 863 (w), 855 (w), 838 (w), 824 (w), 799 (s), 776 (w), 766 (m), 741 (w), 698 (w), 683 (w), 655 (w), 640 (m), 610 (w), 587 (w), 545 (w), 519 (w), 502 (w) cm^{-1}. NIR (Nujol): $\tilde{\nu} \approx 2010$ nm.

[$AP_3Ga_2(THF)_2$] (7): A solution of amidophenolatodisodium derivative $APNa_2$[29] (1.3 mmol, 0.55 g) in THF (20 mL) was added to the solution of GaI_3 (0.87 mmol, 0.39 g) in the same solvent (10 mL). A color change from deep yellow to pale yellow was observed. The THF was evaporated and residue was dissolved in pentane (20 mL). The NaI precipitate was removed by filtration. The complex **7** was obtained as a fine-crystalline, nearly colorless product after cooling; yield 0.33 g (53.4%); m.p. (dec.) > 140 °C. $C_{86}H_{127}Ga_2N_3O_5$ (1422.41): calcd. C 72.62, H 9.00, Ga 9.80; found C 72.64, H 9.07, Ga 9.73. ^{1}H NMR (C_6D_6, 20 °C): δ = 7.26 (dd, $^1J_{H,H}$ = 7.63, $^2J_{H,H}$ = 1.53 Hz, 3 H, H_{arom}), 7.17 (t, $^1J_{H,H}$ = 7.63 Hz, 3 H, H_{arom}), 7.09 (dd, $^1J_{H,H}$ = 7.63, $^2J_{H,H}$ = 1.53 Hz, 3 H, H_{arom}), 6.80 (s, $^2J_{H,H}$ = 2.32 Hz, 3 H, H_{arom}), 6.27 (s, $^2J_{H,H}$ = 2.32 Hz, 3 H, H_{arom}), 4.08 [sept., $^1J_{H,H}$ = 6.9, 3 H, CH(*i*Pr)], 3.13 [m, 8 H, CH_2^{α}(THF)], 2.91 [sept., $^1J_{H,H}$ = 6.9, 3 H, CH(*i*Pr)], 1.54 (s, 27 H, *t*Bu), 1.46 [d, $^1J_{H,H}$ = 6.9, 9 H, CH_3(*i*Pr)], 1.34 [d, $^1J_{H,H}$ = 6.9, 9 H, CH_3(*i*Pr)], 1.26 (s, 27 H, *t*Bu), 1.21 [m, 8 H, CH_2^{β}(THF)], 0.96 [d, $^1J_{H,H}$ = 6.9, 9 H, CH_3(*i*Pr)], 0.34 [d, $^1J_{H,H}$ = 6.9, 9 H, CH_3(*i*Pr)] ppm; assignment of NMR spectroscopic signals was defined more exactly by using 2D COSY NMR spectroscopy. IR (Nujol): $\tilde{\nu}$ = 1589 (w), 1562 (m), 1414 (s), 1379 (s), 1359 (s), 1331 (s), 1283 (s), 1264 (s), 1229 (s), 1205 (s), 1117 (m), 1103 (w), 1046 (m), 1030 (w), 986 (s), 942 (m), 935 (w), 907 (w), 900 (w), 858 (w), 843 (w), 814 (m), 799 (m), 765 (m), 760 (m), 745 (w), 717 (m), 682 (m), 654 (w), 612 (w), 586 (w), 547 (m), 531 (m), 507 (m) cm^{-1}.

[{CatGa(I)(THF)}$_2$] (8). Method 1: A solution of **3,6-Q** (2.3 mmol, 0.5 g) in toluene (30 mL) was added to the suspension of "GaI" (2.3 mmol, 0.45 g) in the same solvent (10 mL). The "GaI" precipitate dissolved and a light-yellow solution formed. Compound **8** was obtained after recrystallization from THF/hexane mixture as nearly colorless crystals; yield 0.76 g (67.9%); m.p. (dec.) > 130 °C. $C_{36}H_{56}Ga_2I_2O_6$ (978.08): calcd. C 44.21, H 5.77, Ga 14.26, I 25.95; found C 44.27, H 5.81, Ga 14.21, I 25.90. ^{1}H NMR [$(CD_3)_2O$, 20 °C]: δ = 6.72 (s, 2 H, H_{arom}), 3.62 [m, 4 H, CH_2^{α}(THF)], 1.79 [m, 4 H, CH_2^{β}(THF)], 1.36 (s, 36 H, *t*Bu) ppm. IR (Nujol): $\tilde{\nu}$ = 1394 (s), 1350 (s), 1285 (s), 1261 (s), 1250 (m), 1221 (m), 1196 (m), 1146 (m), 1017 (s), 969 (s), 932 (m), 914 (s), 860 (s), 832 (w), 812 (m), 800 (m), 700 (m), 677 (m), 659 (s), 605 (w), 560 (w), 548 (w) cm^{-1}.

Method 2: A solution of **3,6-Q** (2.3 mmol, 0.5 g) and I_2 (1.15 mmol, 0.29 g) in THF (30 mL) was added to the excess amount of gallium (12 mmol, 0.84 g). The reaction mixture was stirred and heated until the solution turned pale yellow. The solution was separated from the excess amount of metal. The fine-crystalline product **8** was obtained after recrystallization from a mixture of THF/hexane; yield 0.82 g (73.0%).

[AP_2Ga][GaI_2] (9). Method 1: A solution of **imQ** (1.3 mmol, 0.5 g) in toluene (30 mL) was added to the suspension of "GaI" (1.3 mmol, 0.256 g) in the same solvent (10 mL). The "GaI" precipitate dissolved, and a pale yellow solution formed. Complex **9** was obtained as a fine-crystalline, pale yellow product after cooling; yield 0.536 g (71.5%); m.p. (dec.) > 150 °C. $C_{52}H_{74}Ga_2I_2N_2O_2$ (1152.42): calcd. C 54.20, H 6.47, Ga 12.10, I 22.02; found C 54.23, H 6.51, Ga 12.08, I 22.00. ^{1}H NMR ($CDCl_3$, 20 °C): δ = 7.17–7.14 (m, 4 H, H_{arom}), 6.99–6.93 (m, 2 H, H_{arom}), 6.70 (d, $^2J_{H,H}$ = 2.34 Hz, 2 H, H_{arom}), 5.93 (d, $^2J_{H,H}$ = 2.34 Hz, 2 H, H_{arom}), 3.59 [sept., $^1J_{H,H}$ = 6.9, 2 H, CH(*i*Pr)], 2.37 [sept., $^1J_{H,H}$ = 6.9, 2 H, CH(*i*Pr)], 1.56 (s, 18 H, *t*Bu), 1.15 [d, $^1J_{H,H}$ = 6.9, 6 H, CH_3(*i*Pr)], 1.14 [d, $^1J_{H,H}$ = 6.9, 6 H, CH_3(*i*Pr)], 1.07 (s, 18 H, *t*Bu), 0.73 [d, $^1J_{H,H}$ = 6.9, 6 H, CH_3(*i*Pr)], 0.01 [d, $^1J_{H,H}$ = 6.9, 6 H, CH_3(*i*Pr)] ppm. IR (Nujol): $\tilde{\nu}$ = 1589 (m), 1573 (s), 1449 (s), 1407 (s), 1393 (m), 1362 (s), 1323 (s), 1283 (s), 1262 (m), 1257 (m), 1238 (m), 1220 (w), 1199 (m), 1189 (s), 1151 (m), 1111 (m), 1096 (s), 1054 (w), 1042 (w), 1026 (w), 986 (s), 955 (w), 939 (w), 935 (w), 927 (w), 901 (w), 861 (w), 850 (w), 813 (m), 801 (s), 769 (w), 750 (w), 740 (w), 662 (w), 653 (w), 583 (w), 547 (w), 533 (w), 508 (w), 476 (w) cm^{-1}.

Method 2: A solution of **imQ** (1.3 mmol, 0.5 g) and I_2 (0.65 mmol, 0.165 g) in toluene (30 mL) was added to an excess amount of gallium (12 mmol, 0.84 g). The reaction mixture was stirred until the solution turned pale yellow. The solution was separated from the excess amount of metal. Complex **9** was obtained as a fine-crystalline, pale yellow product after cooling; yield 0.519 g (69.2%).

CCDC-882125 (for **3**) and -882126 (for **9**) contain the supplementary crystallographic data for this paper. These data can be obtained free of charge from The Cambridge Crystallographic Data Centre via www.ccdc.cam.ac.uk/data_request/cif.

Acknowledgments

We are grateful to the FSP Scientific and Scientific-Pedagogical Cadres of Innovation Russia for the years 2009–2013 (GK P839 from 25.05.2010), the Russian Foundation for Basic Research (grant number 10-03-00788), and the Russian President Grants (NSh-1113.2012.3, MK-614.2011.3) for financial support of this work.

[1] W. I. Dzik, J. I. van der Vlugt, J. N. H. Reek, B. de Bruin, *Angew. Chem.* **2011**, *123*, 3416; *Angew. Chem. Int. Ed.* **2011**, *50*, 3356–3358.

[2] a) G. A. Abakumov, A. I. Poddel'sky, E. V. Grunova, V. K. Cherkasov, G. K. Fukin, Yu. A. Kurskii, L. G. Abakumova, *Angew. Chem.* **2005**, *117*, 2827; *Angew. Chem. Int. Ed.* **2005**, *44*, 2767–2771; b) V. K. Cherkasov, G. A. Abakumov, E. V. Grunova, A. I. Poddel'sky, G. K. Fukin, E. V. Baranov, Yu. A. Kursky, L. G. Abakumova, *Chem. Eur. J.* **2006**, *12*, 3916–3927; c) A. V. Lado, A. V. Piskunov, V. K. Cherkasov, G. K. Fukin, G. A. Abakumov, *Russ. J. Coord. Chem.* **2006**, *32*, 173–180; d) A. V. Piskunov, A. I. Aivaz'yan, V. K. Cherkasov, G. A. Abakumov, *J. Organomet. Chem.* **2006**, *691*, 1531–1534; e) G. A. Abakumov, V. K. Cherkasov, A. V. Piskunov, A. V. Lado, G. K. Fukin, L. G. Abakumova, *Russ. Chem. Bull.* **2006**, *55*, 1146–1154; f) A. V. Piskunov, I. N. Mescheryakova, G. K. Fukin, E. V. Baranov, M. Hummert, A. S. Shavyrin, V. K. Cherkasov, G. A. Abakumov, *Chem. Eur. J.* **2008**, *14*, 10085–10093.

[3] a) I. L. Fedushkin, A. A. Skatova, M. Hummert, H. Schumann, *Eur. J. Inorg. Chem.* **2005**, 1601–1608; b) E. V. Kolyakina, L. B. Vaganova, A. V. Piskunov, A. V. Lado, V. K. Cherkasov, D. F. Grishin, *Russ. Chem. Bull.* **2007**, *56*, 1363–1368; c) E. V. Kolyakina, L. B. Vaganova, A. V. Piskunov, A. V. Lado, V. K. Cherkasov, D. F. Grishin, *Polym. Sci., Ser. A* **2008**, *50*, 153–159; d) E. V. Kolyakina, L. B. Vaganova, A. V. Piskunov, A. V. Lado, D. F. Grishin, *Polym. Sci., Ser. B* **2009**, *51*, 96–101.

[4] a) I. L. Fedushkin, A. S. Nikipelov, K. A. Lyssenko, *J. Am. Chem. Soc.* **2010**, *132*, 7874–7875; b) I. L. Fedushkin, A. S. Nikipelov, A. G. Morozov, A. A. Skatova, A. V. Cherkasov, G. A. Abakumov, *Chem. Eur. J.* **2012**, *18*, 255–266.

[5] a) G. A. Razuvaev, G. A. Abakumov, E. S. Klimov, *Dokl. Akad. Nauk SSSR* **1971**, *201*, 624–627; b) G. A. Abakumov, E. S. Klimov, *Dokl. Akad. Nauk SSSR* **1972**, *202*, 827–829; c) G. A. Abakumov, E. S. Klimov, V. V. Ershov, I. S. Belostotskaya, *Russ. Chem. Bull.* **1975**, *24*, 841–843; d) E. S. Klimov, A. V. Lobanov, G. A. Abakumov, *Russ. Chem. Bull.* **1981**, *30*, 1664–1666.

[6] M. A. Brown, A. A. El-Hadad, B. R. McGarvey, R. C. W. Sung, A. K. Trikha, D. G. Tuck, *Inorg. Chim. Acta* **2000**, *300–302*, 613–621.

[7] G. A. Razuvaev, G. A. Abakumov, E. S. Klimov, E. N. Gladyshev, P. Ya. Bayushkin, *Russ. Chem. Bull.* **1977**, *26*, 1034–1037.

[8] A. V. Piskunov, A. I. Poddel'sky, *Glob. J. Inorg. Chem.* **2011**, *2*, 110–149.

[9] a) I. L. Fedushkin, A. N. Lukoyanov, A. N. Tishkina, G. K. Fukin, K. A. Lyssenko, M. Hummert, *Chem. Eur. J.* **2010**, *16*, 7563–7571; b) A. I. Prokof'ev, N. N. Bubnov, S. P. Solodovnikov, M. I. Kabachnik, *Dokl. Akad. Nauk SSSR* **1979**, *245*, 1123–1126; c) A. Ozarowsky, B. R. McGarvey, A. A. El-Hadad, Z. Tian, D. G. Tuck, D. J. Krovich, G. C. DeFotis, *Inorg. Chem.* **1993**, *32*, 841–847; d) D. M. Adams, A. L. Reingold, A. Dei, D. N. Hendrickson, *Angew. Chem.* **1993**, *105*, 434–436.

[10] a) T. A. Annan, D. G. Tuck, *Can. J. Chem.* **1989**, *67*, 1807–1814; b) Y. G. Lawson, N. C. Norman, A. G. Orpen, M. J. Quayle, *Acta Crystallogr., Sect. C* **1997**, *53*, 1805–1809.

[11] a) S. P. Green, C. Jones, A. Stasch, R. P. Rose, *New J. Chem.* **2007**, *31*, 127–134; b) T. Pott, P. Jutzi, W. Kaim, W. W. Schoeller, B. Neumann, A. Stammler, H. G. Stammler, M. Wanner, *Organometallics* **2002**, *21*, 3169–3172; c) R. J. Baker, R. D. Farley, C. Jones, M. Kloth, D. M. Murphy, *J. Chem. Soc., Dalton Trans.* **2002**, 3844–3850; d) R. J. Baker, C. Jones, M. Kloth, D. P. Mills, *New J. Chem.* **2004**, *28*, 207–213; e) R. J. Baker, C. Jones, *Dalton Trans.* **2005**, 1341–1348; f) T. Jurca, K. Dawson, I. Mallov, T. Burchell, G. P. A. Yap, D. S. Richeson, *Dalton Trans.* **2010**, *39*, 1266–1272.

[12] a) P. Chaudhuri, R. Wagner, U. Pieper, B. Biswas, T. Weyhermuller, *Dalton Trans.* **2008**, 1286–1288; b) P. Chaudhuri, E. Bill, R. Wagner, U. Pieper, B. Biswas, T. Weyhermuller, *Inorg. Chem.* **2008**, *47*, 5549–5551.

[13] C. W. Lange, B. J. Conclin, C. G. Pierpont, *Inorg. Chem.* **1994**, *33*, 1276–1283.

[14] S. S. Batsanov, *Russ. J. Inorg. Chem.* **1991**, *36*, 1694–1706.

[15] J. Emsley, *The Elements*, Clarendon Press, Oxford, UK, **1991**, p. 251.

[16] A. V. Piskunov, I. N. Mescheryakova, E. V. Baranov, G. K. Fukin, V. K. Cherkasov, G. A. Abakumov, *Russ. Chem. Bull.* **2010**, *59*, 361–370.

[17] A. V. Piskunov, I. A. Aivaz'yan, A. I. Poddel'sky, G. K. Fukin, E. V. Baranov, V. K. Cherkasov, G. A. Abakumov, *Eur. J. Inorg. Chem.* **2008**, 1435–1444.

[18] H. M. Tuononen, A. F. Armstrong, *Dalton Trans.* **2006**, 1885–1894.

[19] a) A. V. Piskunov, A. V. Maleeva, G. K. Fukin, E. V. Baranov, O. V. Kuznetsova, *Russ. J. Coord. Chem.* **2010**, *36*, 161–169; b) A. V. Piskunov, A. V. Maleeva, G. K. Fukin, A. S. Bogomyakov, V. K. Cherkasov, G. A. Abakumov, *Dalton Trans.* **2011**, *40*, 718–725.

[20] a) A. I. Poddelsky, V. K. Cherkasov, G. A. Abakumov, *Coord. Chem. Rev.* **2009**, *253*, 291–324; b) S. N. Brown, *Inorg. Chem.* **2012**, *51*, 1251–1260.

[21] D. D. Perrin, W. L. F. Armarego, D. R. Perrin, *Purification of Laboratory Chemicals*, Pergamon Press, Oxford, **1980**, p. 391.

[22] V. A. Garnov, V. I. Nevodchikov, L. G. Abakumova, G. A. Abakumov, V. K. Cherkasov, *Russ. Chem. Bull.* **1987**, *36*, 1728–1729.

[23] G. A. Abakumov, N. O. Druzhkov, Yu. A. Kurskii, A. S. Shavyrin, *Russ. Chem. Bull.* **2003**, *52*, 712–717.

[24] B. Freeland, D. G. Tuck, *Inorg. Chem.* **1976**, *15*, 475–476.

[25] M. L. H. Green, P. Mountford, G. J. Smout, S. R. Speel, *Polyhedron* **1990**, *9*, 2763–2765.

[26] Bruker, *SAINTPLUS*, *Data Reduction and Correction Program*, v. 6.02a, Bruker AXS, Madison, WI, USA, **2000**.

[27] G. M. Sheldrick, *SADABS*, v. 2.01, *Area Detector Absorption Correction Program*, Bruker AXS, Madison, WI, USA, **1998**.

[28] G. M. Sheldrick, *SHELXTL*, v. 6.12, *Structure Determination Software Suite*, Bruker AXS, Madison, WI, USA, **2000**.

[29] A. V. Piskunov, I. N. Mescheryakova, A. S. Bogomyakov, G. V. Romanenko, V. K. Cherkasov, G. A. Abakumov, *Inorg. Chem. Commun.* **2009**, *12*, 1067–1070.

Received: May 17, 2012
Published Online: ■

Redox-Active Ligands

The reduction of sterically hindered *o*-benzo- and *o*-iminobenzoquinone with gallium as well as with "GaI" was found to be a versatile method for the synthesis of gallium complexes that are based on these redox-active ligands. The described reactions allowed metal derivatives that contain differently charged organic ligands to be obtained depending on the reaction conditions.

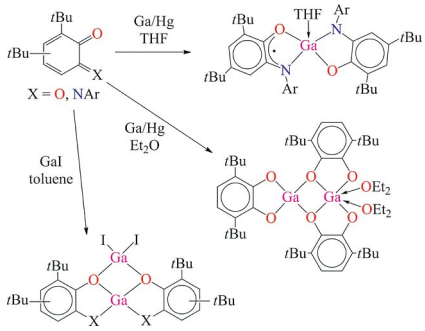

Keywords: Gallium / Quinones / Reduction / EPR spectroscopy

